

Supporting Information

Earls et al. 10.1073/pnas.0910630107

SI Materials and Methods

Strain List. NC1400 *pRN2003[pdat-1::GFP rol-6(su1006)]; juIs96 [punc-25::GFP lin-15(+)]; eri-1(mg366); lin-15B(n744)*
NC1404 *juIs14[pacr-2::GFP lin-15(+)]; eri-1(mg366); lin-15B(n744)*
NC1405 *juIs96[punc-25::GFP lin-15(+)]; eri-1(mg366); lin-15B(n744)*
NC1407 *juIs96[punc-25::GFP lin-15(+)]; ced-4(n1162); eri-1(mg366); lin-15B(n744)*
NC1420 *myo-3(st386); eri-1(mg366); lin-15B(n744); stEx30 [myo-3::GFP rol-6(su1006)]*
NC1436 *adIs1240[eat-4::GFP lin-15(+)]; eri-1(mg366); lin-15B(n744)*
NC1437 *juIs96[punc-25::GFP lin-15(+)]; eri-1(mg366); crt-1(bz30); lin-15B(n744)*
NC1439 *mgIs42[tph-1::GFP rol-6(su1006)]; eri-1(mg366); lin-15B(n744)*
NC1758 *juIs96[punc-25::GFP lin-15(+)]; ced-9(n1950); eri-1(mg366)*
NC1778 *juIs96[punc-25::GFP lin-15(+)]; eri-1(mg366) drp-1(tm1108)*
NC1635 *coq-1(ok749)/dpy-5(e61); juIs14[acr-2::GFP lin-15(+)]*
NC1660 *coq-1(ok749)/dpy-5(e61); juIs96[punc-25::GFP lin-15(+)]*
NC1647 *juIs96[punc-25::GFP lin-15(+)]; eri-1(mg366) ced-3(n717)*
NC1941 *juIs96[punc-25::GFP lin-15(+)]; eri-1(mg366); egl-1(n1084n3082)*
NC1959 *juIs96[punc-25::GFP lin-15(+)]; coq-2(ok1066)/hT2*
NC1974 *juIs96[punc-25::GFP lin-15(+)]; coq-3(ok506)/nT1*
NC1993 *coq-2(ok1066)/hT2; juIs14[pacr-2::GFP lin-15(+)]*
NC1999 *juIs96[punc-25::GFP lin-15(+)]; ced-4(n1162); coq-3(ok506)/nT1*
NC2020 *coq-2(ok1066)/hT2; juIs14[pacr-2::GFP lin-15(+)]; wdEx658[punc-25::mcherry unc-119(+)]*
NC2026 *juIs96[punc-25::GFP lin-15(+)]; eri-1(mg366); egl-1(ok1418)*

Strain Maintenance. N2 (wild-type), *ced-3(n717)*, *ced-4(n1162)*, *ced-9(n1950gf)*, *coq-1(ok749)*, *coq-2(ok1066)*, *coq-3(ok506)*, *crt-1(bz30)*, *egl-1(ok1418)*, and *egl-1(n1084n3082)*, and the GFP reporter strains *acr-2::GFP(juIs14)* (1), *eat-4::GFP(adIs1240)* (2), *myo-3::MYO-3-GFP(stEx30)* (3), *unc-25::GFP(juIs76)* (4), and *tph-1::GFP(mgIs42)* (5) were obtained from the Caenorhabditis Genetics Center (University of Minnesota, Minneapolis, MN). *drp-1(tm1108)* was provided by D. Xue (University of Colorado, Boulder, CO) (6). *pdat-1::GFP(pRN2003)* was obtained from R. Blakely (Vanderbilt University, Nashville, TN) (7). *coq-1(ok749)* was outcrossed four times, maintained in trans to *dpy-5(e61)*, and genotyped by PCR: 5'-catgaatttagcagcaatgac (forward), 5'-cttcacgcagaggtcagagtg (reverse), 5'-ccaactgctgacgatctcttg (poison). PCR conditions were as

follows: denaturing, 94 °C for 5 min; cycling, 94 °C for 30 s, 50 °C for 45 s, 72 °C for 3 min, 35 times; final extension, 72 °C for 7 min. *coq-1* wild-type bands are 2.5 kb and ≈900 bp and *coq-1* mutant band is ≈600 bp. *coq-1(ok749)*; *unc-25::GFP(juIs76)* and *coq-1(ok749)*; *acr-2::GFP(juIs14)* animals were used to examine GABA and cholinergic neurons in *coq-1* mutant animals, respectively.

GABA neuron degeneration was observed in *coq-1(ok749)* maintained at 15 °C. *egl-1(ok1418)*, *egl-1(n1084n3082)*, and *ced-9(n1950)* were verified by sequencing in *eri-1(mg366)*; *unc-25::GFP(juIs76)* genetic backgrounds. Cholinergic neurons marked with *acr-2::GFP* (1) were quantified in the same manner, and no significant degeneration was detected. Additional neuron classes were examined (S4), but no differences between control (empty vector) and *coq-1* RNAi knockdown animals were observed in these neurons. For GFP knockdown in reporter strains (S4), quantification of fluorescence in Z series of confocal optically sectioned images was done by using histogram analysis in ImageJ (8).

pMLH41 was constructed by ligating a 1.8-kb PCR amplicon of the *unc-25* promoter from pSC392 (a generous gift from Yishi Jin, University of California, San Diego, CA) into *punc-4::mcherry* (9) by using 5'-SphI and 3'-AscI. The *unc-119* minigene from pDP#MM051 (10) was inserted into the vector backbone between PacI and ApaI.

PCR Assay To Detect *eri-1(mg366)*. Single-worm PCR was performed with primers 5'-gataaaacttcggaacatattggggc (forward) and 5'-actgatggtaaggaatcgaagacg (reverse); the *eri-1* PCR amplicon (223 bp) is distinguishable on a 2% agarose gel from the wild-type band (200 bp). *eri-1 ced-3* recombinants were created by crossing *eri-1 unc-22* heterozygous males into *ced-3* hermaphrodites. Non-Unc animals were PCR-genotyped for *eri-1/eri-1*, and animals lacking *unc-22* progeny were verified by sequencing as *eri-1 ced-3* (11).

Treatments with Coenzyme Q (CoQ). CoQ₁₀ (Sigma) was dissolved in 0.06% Tween-80 (12) and added to media before pouring plates. Tween-80 (0.06%) alone had no effect on degeneration and was used as the normalization control for those experiments.

Combinatorial RNAi

Cultures for combinatorial-RNAi experiments (i.e., *coq-1 + drp-1*, *coq-1 + kap-1*, *coq-1 + fzo-1*) were grown separately and then mixed before plating. *kap-1* is an unrelated gene that has no visible phenotype by RNAi and was used as a control for potential competitive effects of combining two RNAi constructs (Fig. S8).

ATP Measurement

Crude mitochondria were isolated from lysates (13) obtained from a mixed population of *eri-1*; *unc-25::GFP(juIs76)* animals treated with either empty vector (EV) or *coq-1* RNAi. A Roche Cell-Titer Glow Luminescent Cell Viability Assay kit was used to measure ATP levels with a FluorStar Optima luminometer. ATP levels were normalized to protein concentrations and represented in arbitrary units. A Bio-Rad protein assay kit was used to measure protein concentrations in a BioRad3 spectrophotometer. Each measurement was replicated in three independent experiments.

1. Hallam S, Singer E, Waring D, Jin Y (2000) The C. elegans NeuroD homolog *cnd-1* functions in multiple aspects of motor neuron fate specification. *Development* 127: 4239–4252.
2. Lee RY, Sawin ER, Chalfie M, Horvitz HR, Avery L (1999) EAT-4, a homolog of a mammalian sodium-dependent inorganic phosphate cotransporter, is necessary for glutamatergic neurotransmission in caenorhabditis elegans. *J Neurosci* 19:159–167.

3. Campagnola PJ, et al. (2002) Three-dimensional high-resolution second-harmonic generation imaging of endogenous structural proteins in biological tissues. *Biophys J* 82:493–508.
4. Jin Y, Jorgensen E, Hartwig E, Horvitz HR (1999) The Caenorhabditis elegans gene *unc-25* encodes glutamic acid decarboxylase and is required for synaptic transmission but not synaptic development. *J Neurosci* 19:539–548.

- Sze JY, Victor M, Loer C, Shi Y, Ruvkun G (2000) Food and metabolic signalling defects in a *Caenorhabditis elegans* serotonin-synthesis mutant. *Nature* 403:560–564.
- Breckenridge DG, et al. (2008) *Caenorhabditis elegans* drp-1 and fis-2 regulate distinct cell-death execution pathways downstream of ced-3 and independent of ced-9. *Mol Cell* 31:586–597.
- Nass R, Hall DH, Miller DM 3rd, Blakely RD (2002) Neurotoxin-induced degeneration of dopamine neurons in *Caenorhabditis elegans*. *Proc Natl Acad Sci USA* 99:3264–3269.
- Rasband WSI (1997–2007) *ImageJ* (US Natl Inst Health, Bethesda, MD).
- Feinberg EH, et al. (2008) GFP Reconstitution Across Synaptic Partners (GRASP) defines cell contacts and synapses in living nervous systems. *Neuron* 57:353–363.
- Maduro M, Pilgrim D (1995) Identification and cloning of unc-119, a gene expressed in the *Caenorhabditis elegans* nervous system. *Genetics* 141:977–988.
- Shaham S, Reddien PW, Davies B, Horvitz HR (1999) Mutational analysis of the *Caenorhabditis elegans* cell-death gene ced-3. *Genetics* 153:1655–1671.
- Ishii N, et al. (2004) Coenzyme Q10 can prolong *C. elegans* lifespan by lowering oxidative stress. *Mech Ageing Dev* 124:41–46.
- Grad LI, Sayles LC, Lemire BD (2007) Isolation and functional analysis of mitochondria from the nematode *Caenorhabditis elegans*. *Methods Mol Biol* 372:51–66.

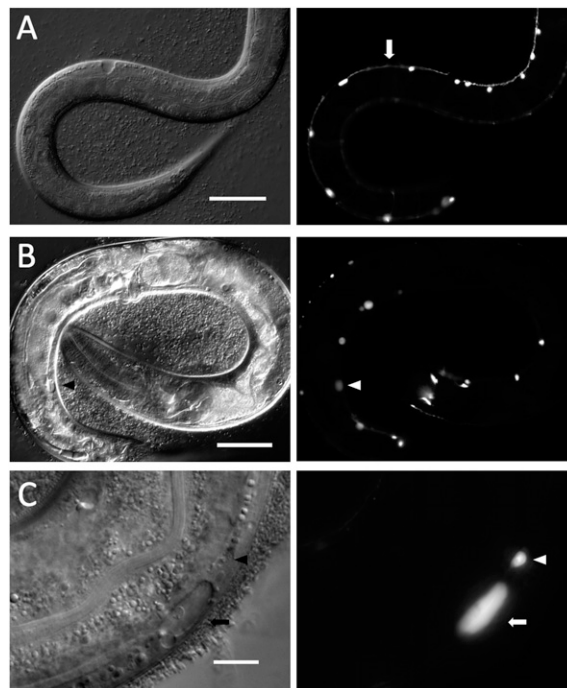


Fig. S1. GABA neuron degeneration in *coq-1(ok749)* animals. DIC (Left) and GFP (Right) views of *unc-25::GFP*-labeled GABA neurons in *coq-1(ok749)* at the L3 (A) and adult (B) stages. Arrow denotes intact ventral nerve cord (VNC) in L3 larva (A) and arrowhead marks swollen GABAergic motor neuron cell body in adult (B). (C) Enlarged (arrow) and normal (arrowhead) GABAergic cell bodies in the VNC. (Scale bars: A and B, 20 μm ; C, 10 μm .)

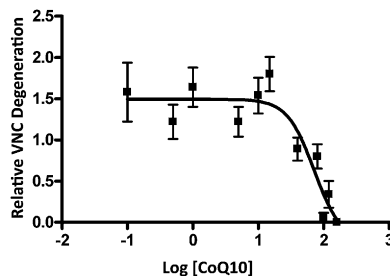


Fig. S2. *coq-1* RNAi-induced GABA neuron degeneration is rescued by treatment with exogenous CoQ₁₀. Dose–response curve showing rescue of GABA neuron degeneration with exogenous CoQ₁₀ ($n = 30$, three independent experiments). $EC_{50} = 72$ mg/mL. After 5 d of RNAi treatment, animals were scored for percent VNC degeneration as in Fig. 2. Relative VNC degeneration was calculated by normalizing percent degeneration at each concentration of CoQ₁₀ to percent degeneration in Tween-80 alone control plates for each separate experiment.

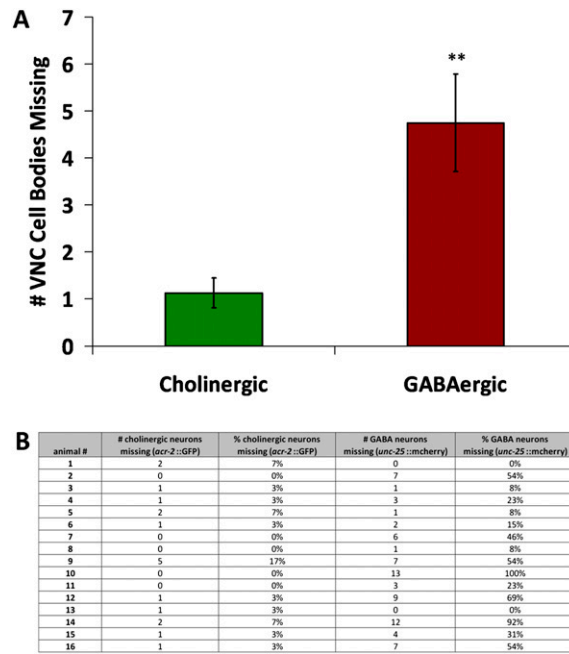


Fig. S3. GABA neurons are more sensitive than neighboring cholinergic neurons to *coq-2* depletion. (A) The number of absent cholinergic (*acr-2::GFP*) and GABAergic (*unc-25::mcherry*) neurons (VA2-VA11 and VD3-VD11, respectively) in adult *coq-2* animals. $**P < 0.002$; $n = 16$. (B) Original data collected for Fig. 2K and Fig. S3A.

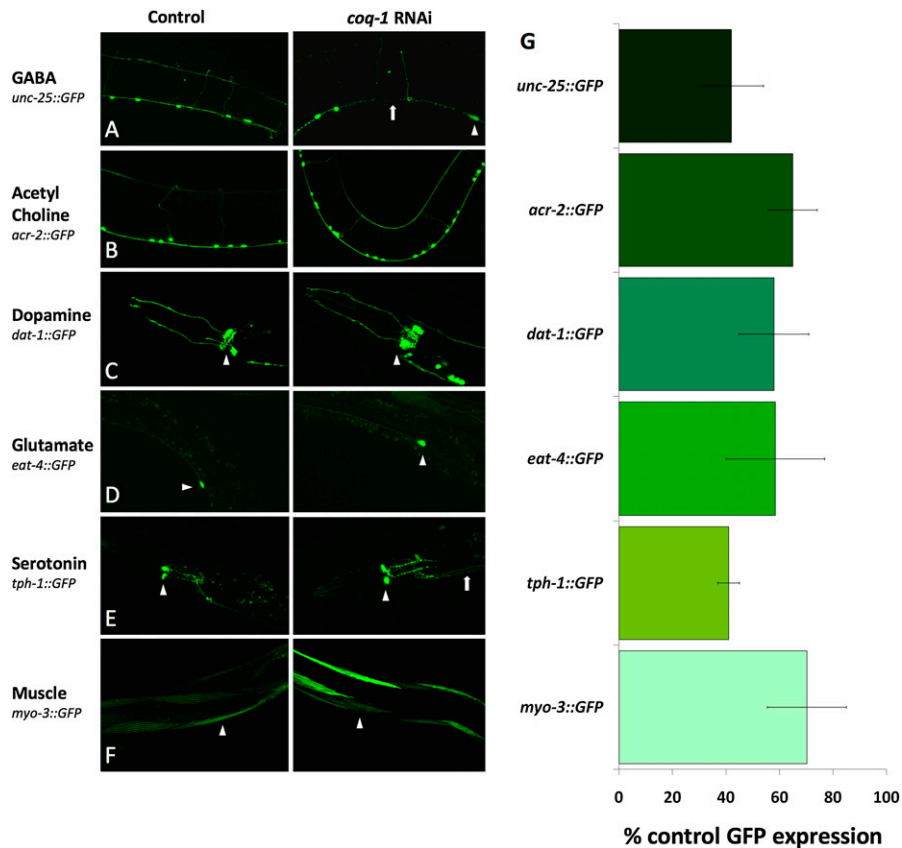


Fig. 54. *coq-1* RNAi triggers preferential degeneration of GABA neurons. Confocal images (40 \times) of empty vector treated control or *coq-1* RNAi-treated animals expressing GFP reporters specific for different neurotransmitter classes of neurons. (A) GABAergic neurons detected by *unc-25::GFP*. *coq-1* RNAi-treated animals show both VNC degeneration (arrow) and swollen neurons (arrowhead). Other classes of neurons and muscle cells do not show degeneration in age-matched animals subject to *coq-1* RNAi-treatment for the same period. (B) Cholinergic neurons, *acr-2::GFP*. (C) Dopaminergic neurons, *dat-1::GFP*. Arrowhead, CEP neuron. (D) Glutamatergic neurons, *eat-4::GFP*. Arrowheads point to AVM (Left) and ALM (Right). (E) Serotonergic neurons, *tph-1::GFP*. NSM cell body (arrowheads) and HSN axonal projection (arrow) are shown. (F) Muscle, *myo-3::GFP*. Arrowheads point to body wall muscle cells. (G) Sensitivity to RNAi knockdown in each GFP-labeled cell type was determined by measuring GFP fluorescence after RNAi against GFP. GFP fluorescence intensity values were obtained from a through focus Z-series collected in a confocal microscope and quantified by histogram analysis in ImageJ ($n = 6$, avg \pm SD). Fluorescence intensities for each GFP strain were normalized to measurements obtained from a control (RNAi with empty vector) to calculate % control GFP expression.

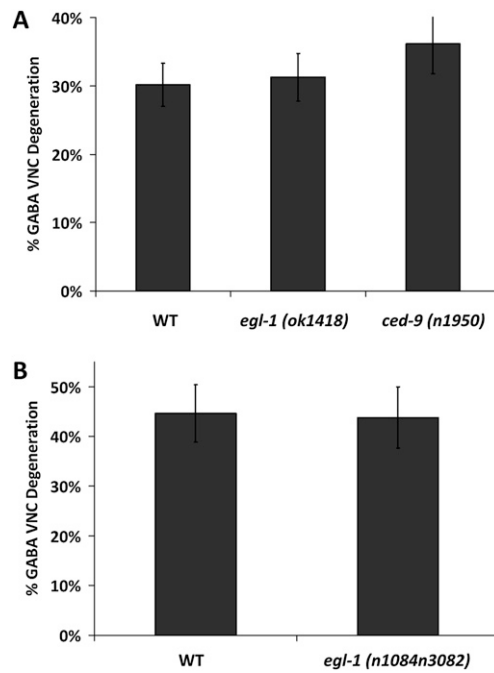


Fig. S5. Apoptotic genes *egl-1* and *ced-9* are not required for *coq-1* RNAi-induced GABA neuron degeneration. (A) *egl-1(ok1418)* and *ced-9(n1950)* were assayed for GABA neuron degeneration after *coq-1* knockdown as in Fig. 2 ($n > 40$). Results with *egl-1* and *ced-9* do not differ significantly from the wild-type control in these experiments. (B) In a separate experiment, another *egl-1* loss-of-function allele, *n1084n3082*, was treated with *coq-1* RNAi and assayed for GABA neuron degeneration ($n > 20$), with no significant difference from the wild-type control.

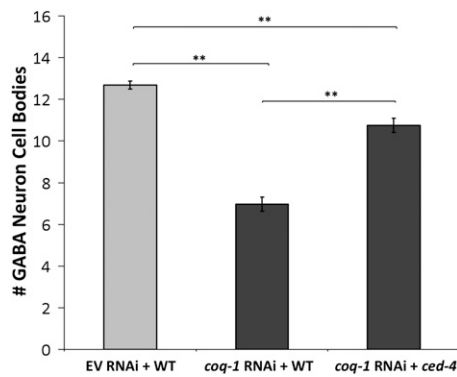


Fig. S6. *ced-4* suppresses degeneration of GABA neuron cell bodies in *coq-1* RNAi-treated animals. *unc-25::GFP*-positive GABA neurons in the VNC interval from VD3-DD11 (13 total cells) were counted for *coq-1* RNAi-treated wild-type (WT) and *ced-4(n1162)* and for the negative control of wild-type treated with empty vector (EV RNAi + WT), $**P < 0.0001$, $n > 50$. All strains include the *eri-1(mg366)* mutant allele.

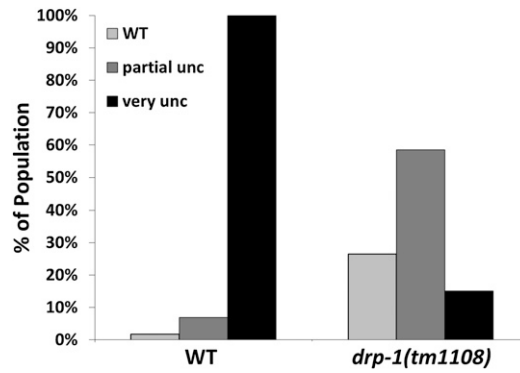


Fig. S7. Uncoordinated (Unc) movement induced by *coq-1* RNAi is suppressed by *drp-1*. Movement assay of wild-type (WT) and *drp-1(tm1108)* mutant animals treated with *coq-1* RNAi. Results shown here were obtained from *coq-1* RNAi-treated animals containing *unc-25::GFP; eri-1(mg366)*. Adults were tapped once on the head and the tail and scored for movement: “partial unc” represents worms that exhibit uncoordinated movement, and “very unc” indicates worms that are unable to move. $n > 100$.

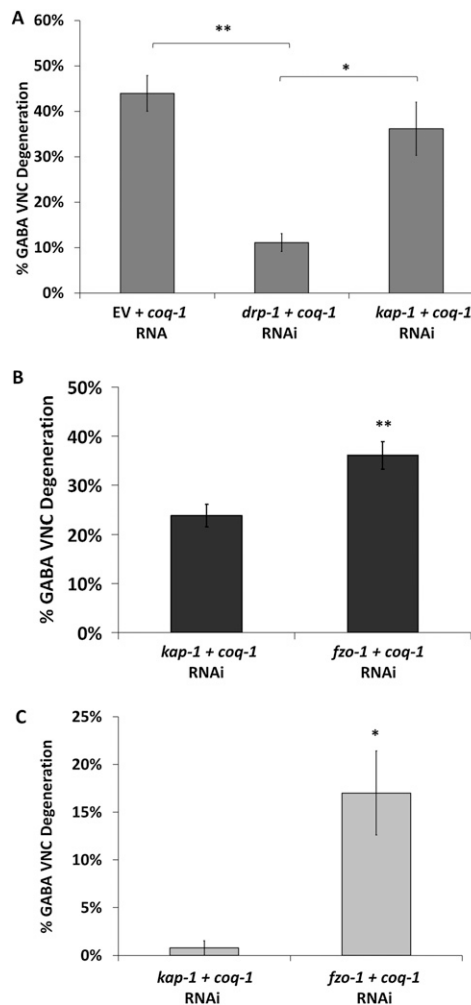


Fig. S8. RNAi of mitochondrial fission and fusion genes influences GABA neuron degeneration induced by *coq-1* RNAi. (A) Double RNAi with empty vector (EV) and *coq-1* results in GABA neuron degeneration ($\approx 44\%$). Double RNAi of *coq-1* with the mitochondrial fission gene *drp-1* results in significantly less GABA neuron degeneration than EV + *coq-1* RNAi control. Double RNAi with a randomly selected control gene *kap-1* (kinesin-associated protein) did not inhibit *coq-1* RNAi-induced GABA neuron degeneration. $n = 60$, $**P < 0.0001$; $*P < 0.0003$. (B) Combinatorial RNAi with *fzo-1* (mitochondrial outer membrane fusion gene) and *coq-1* enhance the GABA neurodegeneration observed with *coq-1* and an unrelated gene, *kap-1*, $n > 100$, $**P < 0.0001$. (C) *fzo-1* RNAi enhances *coq-1* knockdown-induced GABA neuron degeneration in animals lacking the RNAi sensitive mutation *eri-1(mg366)*. $n > 15$, $*P < 0.002$ (Student's *t* test).

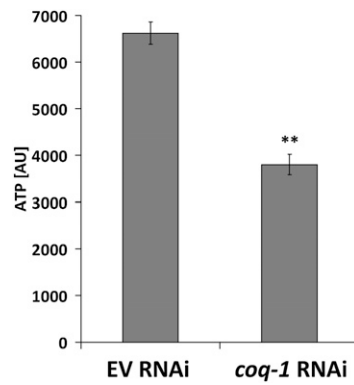


Fig. S9. Mitochondrial ATP levels are reduced in CoQ-depleted animals. ATP levels in mitochondria isolated from whole animal lysates are reduced in *coq-1* RNAi-treated animals versus empty vector-treated control (EV RNAi). ** $P < 0.0008$, $n = 3$. Each sample contained 0.2 μg of total protein. Relative ATP levels are denoted (AU, arbitrary units). ATP levels were measured by using a luminescence assay and normalized to protein concentration (*SI Materials and Methods*).



Movie S1. *coq-1* RNAi induces progressive loss of motor function during larval development. Animals treated with *coq-1* RNAi in early larval stages display wild-type locomotion. As animals progress into late larval (L4) and adult stages, however, body movement is increasingly impaired or uncoordinated (Unc) with older adults appearing largely immobilized.

[Movie S1](#)